Supplementary Data

Supplementary Figures

Figure S1

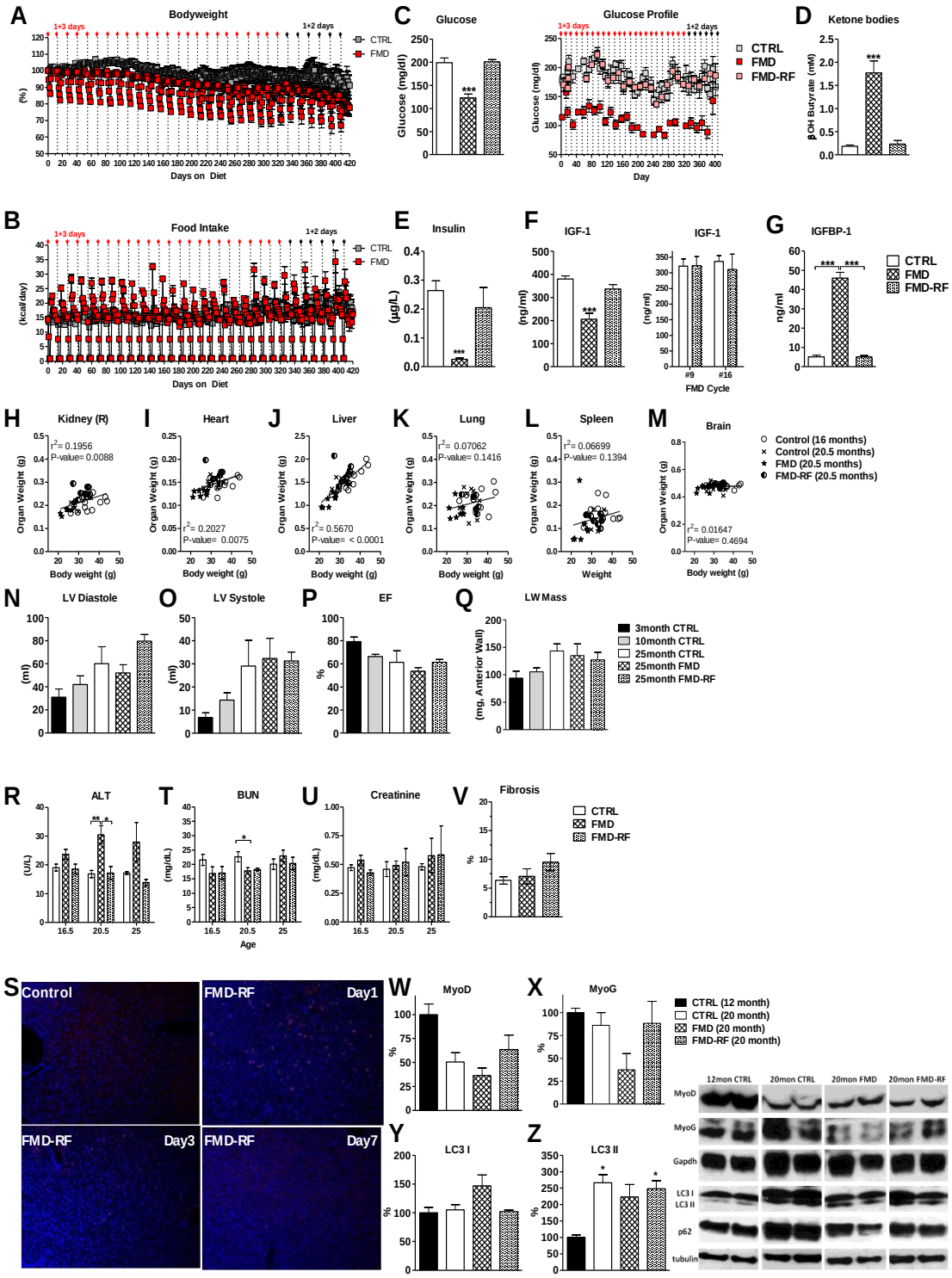

Figure S1 *(Related to Figure 1)*

A) Body weight profile in % compared to the onset of the FMD diet for the *ad lib* fed (gray) and FMD fed (red) cohort. Dashed lines and arrows indicate the onset of the bi-monthly FMD cycle. Red arrows for the 1+3 day feeding cycles, black arrows indicate the 1+2 day schedule later during the study. See text for details. N= 9/group. **B)** Food intake in kcal per day for *ad lib* (gray) and FMD (red) fed groups during the study period. Dashed lines and arrows indicate the onset of the bi-monthly FMD cycle. Red arrows for the 1+3 day feeding cycle, black arrows indicate the 1+2 day schedule later during the study. See text for details. N= 15/group. **C)** Blood glucose (in mg/dL) profile for the *ad lib* fed (gray) and FMD fed (red) cohort. Animals at the end of the FMD cycle in bright red, animals of the FMD group 7 days after re-feeding with normal rodent chow (FMD-RF) in light red. Dashed lines and arrows indicate the onset of the bi-monthly FMD cycle. Red arrows for the 1+3 day feeding cycle, black arrows indicate the 1+2 day schedule later during the study. See text for details. N= 3-5/group. **D)** Ketone bodies, **E)** Serum insulin levels and **F)** Serum insulin-like growth factor (IGF)-1 level in *ad lib* fed control animals, FMD fed and FMD-mice 7 days post re-feeding (FMD-RF) after the first cycle; as well as cycles 9 and 16 for IGF-1. N= 3-5/group. **G)** IGF binding protein-1 (IGFBP-1) measurements for *ad lib* fed control (N= 5) mice or at the end of the FMD feeding cycle (N= 5) at 17 month of age. 7 days after re-feeding, FMD animals were measured again (FMD-RF, N= 5). **H)- M)** Control fed animals were euthanized at 16 months (N= 10) prior to the start of the FMD diet to obtain baseline measurements for organ weight. Comparison of organ weight in relation to body weight for **H)** right kidney, **I)** heart, **J)** liver, **K)** lung, **L)** spleen and **M)** brain. **N)- Q)** Ultrasound echocardiogram data of young (3 months), middle-aged (10 months) and old (25 months) control fed animals as well as 25 months-old animals from the FMD cohort. FMD data obtained on the last day of the dietary regimen, FMD-

RF data 7 days post re-feeding with standard rodent chow. N= 5/group. **N)** Left ventricular (LV) volume in diastole and **O)** systole, **P)** ejection fraction (EJ), and **Q)** the (corrected) relative left ventricular wall (LW) mass were calculated. **R)** Serum alanine transaminase (ALT) level at 16.5, 20.5 and 25 months in control fed and FMD fed mice. For reference, ALT levels 7 days post re-feeding in the FMD cohort are shown (FMD-RF). All data presented as mean ± SEM; * $p<0.05$, ** $p<0.01$, ANOVA, Tukey's multiple comparison. **S)** Liver immunofluorescent staining with Ki67 (red) and DAPI (blue) in control and FMD mice at day 1, 3 and 7 post refeeding. **T)** Serum creatinine and **U)** blood urea nitrogen (BUN) level at 16.5, 20.5 and 25 months in control fed and FMD fed mice. For reference, creatinine and BUN levels 7 days after re-feeding mice in the FMD cohort with normal food are shown (FMD-RF). **V)** Quantification of Masson's trichrome stain to evaluate renal histopathology and glomerular/interstitial fibrosis in control fed mice and animals from the FMD cohort both at the end of diet and the end of re-feeding (FMD-RF). To evaluate myogenesis markers, **W)** MyoD and **X)** MyoG protein expression levels in *ad lib* fed control animals at 12 and 20 months of age in comparison to 20 months-old animal at the end of the FMD dietary cycle or one week after re-feeding (FMD-RF) with normal food were measured. Representative results shown below. N= 4/group. All data presented as mean ± SEM. Protein expression of the autophagy marker **Y)** LC3 I and **Z)** LC3 II was measured in *ad lib* fed control animals at 12 and 20 months of age in comparison to 20 months old animal at the end of the FMD dietary cycle or one week after re-feeding (FMD-RF) with normal food. Representative results shown below. N= 4/group. All data are expressed as the mean ± SEM.

Figure S2

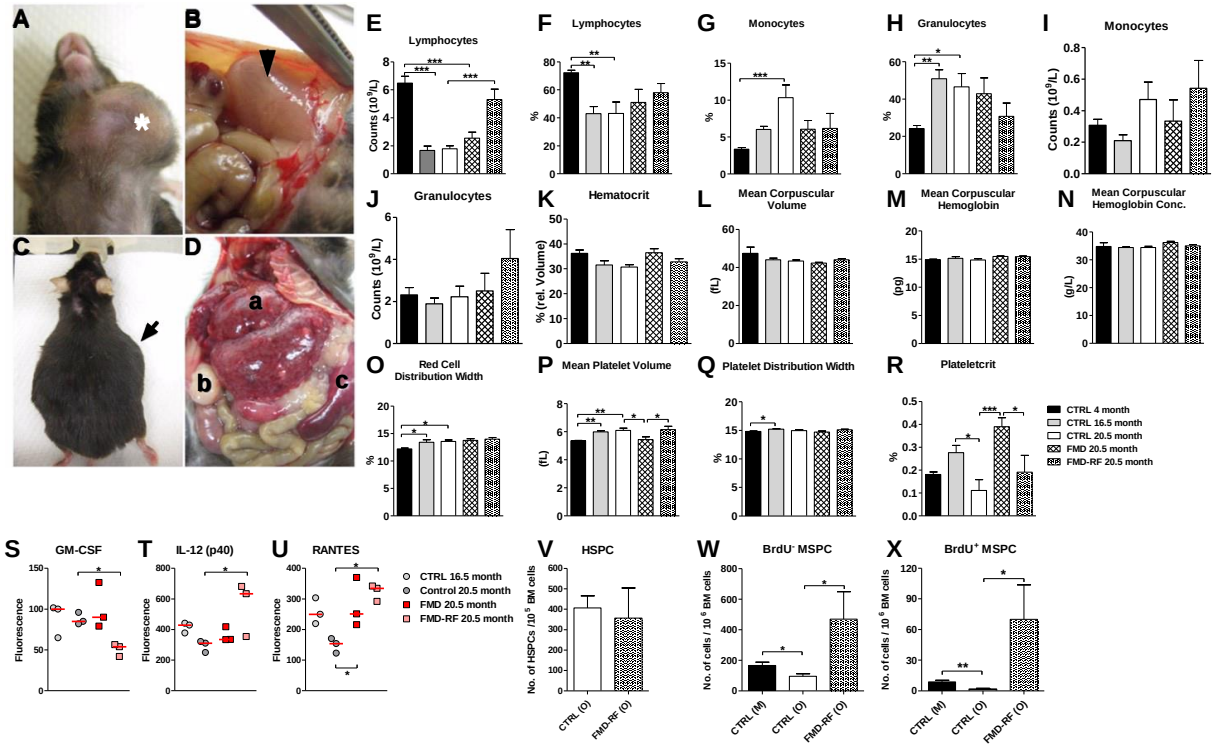

Figure S2 *(Related to Figure 2)*

A) Subcutaneous (*asterisk*) or **C)** internal masses (*arrow*) commonly found in aging animals. The appearance of these masses can be attributed to subcutaneous inflammation with resulting enlarged lymph nodes (**B**, *arrowhead*) or multi-systemic neoplasia (**D**; a: liver, b: ovaries, c: spleen)**. E)-R)** Complete blood counts (CBC) in 4 months, 16.5 months and at 20.5 months-old mice in the *ad lib* fed control and FMD cohort at the end of the FMD dietary cycle or one week after re-feeding (FMD-RF) with normal food were measured. N= 6-10/group. **S)- U)** Significantly changed cytokines out of a panel of 23 markers at age 16.5 months and 20.5 months for CTRL, FMD and FMD-refed animals. **V)** Bone marrow cells were harvested from the femur and tibia of 20.5 months-old control mice and FMD-fed mice 7 days after refeeding (FMD-RF) and stained with lineage-specific Scal-1 (PE-Cy-A) and c-Kit (APC-A) antibodies to measure hematopoietic stem and progenitor cells (HSPC). N= 6/group. All data presented as mean ± SEM. **W) - X)** To detect

the generation of stem/progenitor cells, mice were injected with bromodeoxyuridine (BrdU) 24 hours before bone marrow collection. Bone marrow cells harvested from control fed mature (M, 8-10 month) and old (O, 20.5 month) as well as 20.5 month old FMD-mice 7 days after refeeding (FMD-RF) were sorted by flow cytometry to measure pre-existing ($BrdU^-$) and newly-generated ($BrdU^+$) $Lin^-Sca1^+CD45^-$ mesenchymal stem/progenitor cells (MSPC), also known as very small embryonic like stem cells (VSEL). All data are expressed as the mean ± SEM.

Figure S3

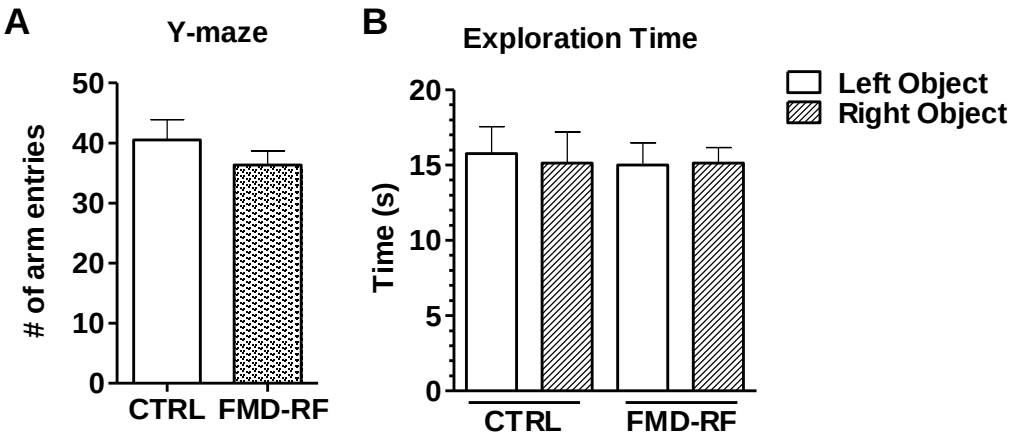

Figure S3 *(Related to Figure 3)*

A) Total number of arm entries of 23 months old (N=11) *ad lib* fed control animals and FMD-mice 7 days after refeeding (FMD-RF) in the Y-maze behavioral test. **B)** Exploration time for the two identical objects placed left and right during the adjustment phase of the novel object recognition task. N= 8/group. All data presented as mean ± SEM.

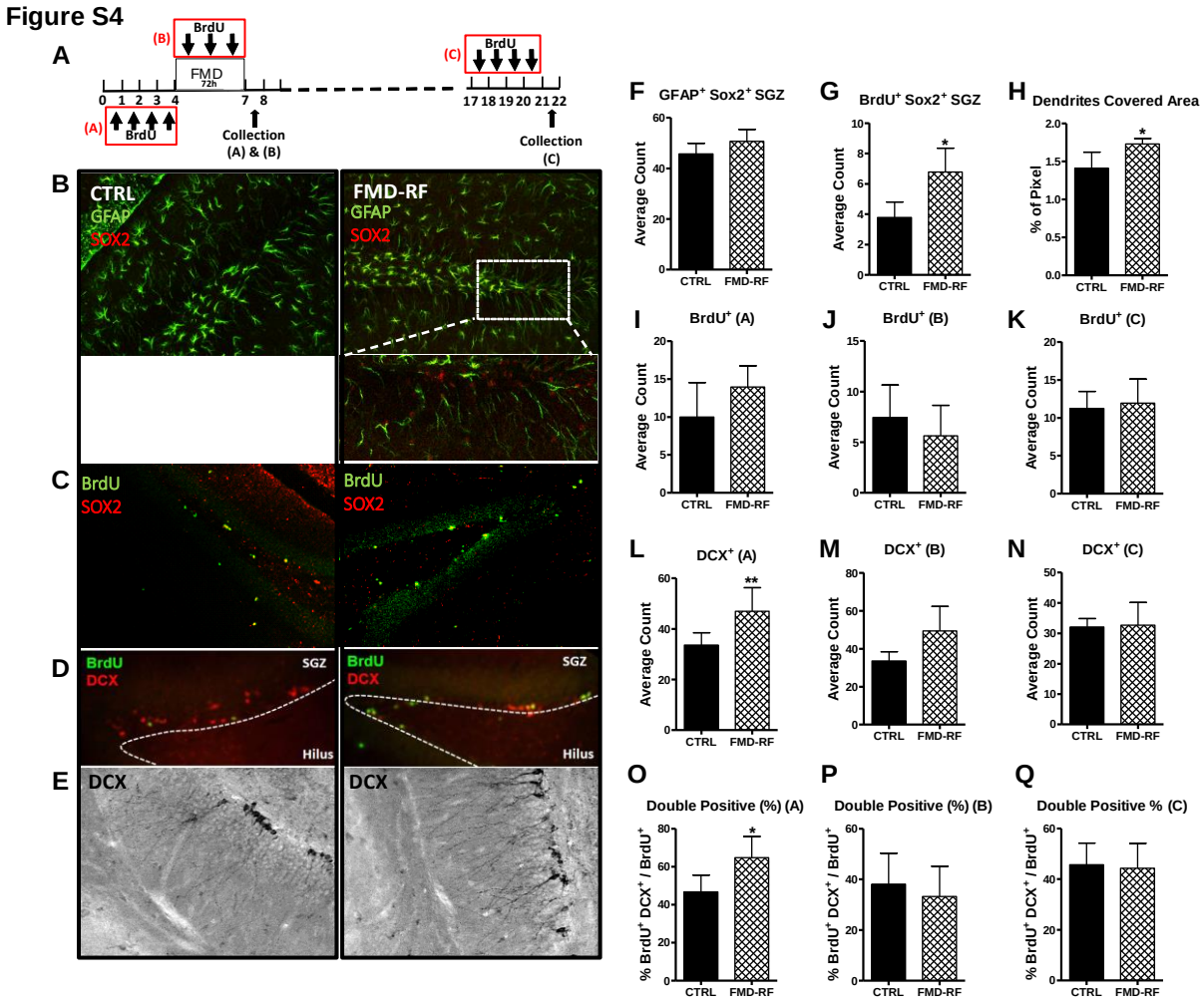

Figure S4 *(Related to Figure 4)*

A) Experimental scheme to assess neural stem cell proliferation and differentiation based on the FMD schedule (*see Methods for details*) and different BrdU injection time points in 6 months-old CD1 mice. **B)** $GFAP^+$ $Sox2^+$ (Type I neural stem cell) in the sub-granular zone (SGZ) in the control group and at the end of FMD (BrdU schedule A). **C)** $BrdU^+$ $Sox2^+$ (Type I and Type II neural stem cell) in SGZ in the control group and at the end of FMD (BrdU schedule B). **D)** $BrdU^+$ DCX^+ in SGZ in the control group and at the end of FMD (BrdU schedule A). **E)** Dendrites (DCX^+, schedule C) covered molecular layer. **F)** Quantification of $GFAP^+$ $Sox2^+$ in SGZ. **G)** $BrdU^+$ $Sox2^+$ in SGZ,

increased BrdU incorporation in $Sox2^+$ cells indicating self-renewal/proliferation of neural stem cell in the FMD cohort (N= 4/group). **H)** Quantification of dendritic covered area of the molecular layer 3 weeks after FMD. **I-Q)** Quantification of $BrdU^+$ (I- H), DCX^+ (L- N) and double positive for $BrdU^+$ DCX^+ over $BrdU^+$ cells (O- Q) at time points A, B and C. All data are expressed as the mean ± SEM.

Figure S5

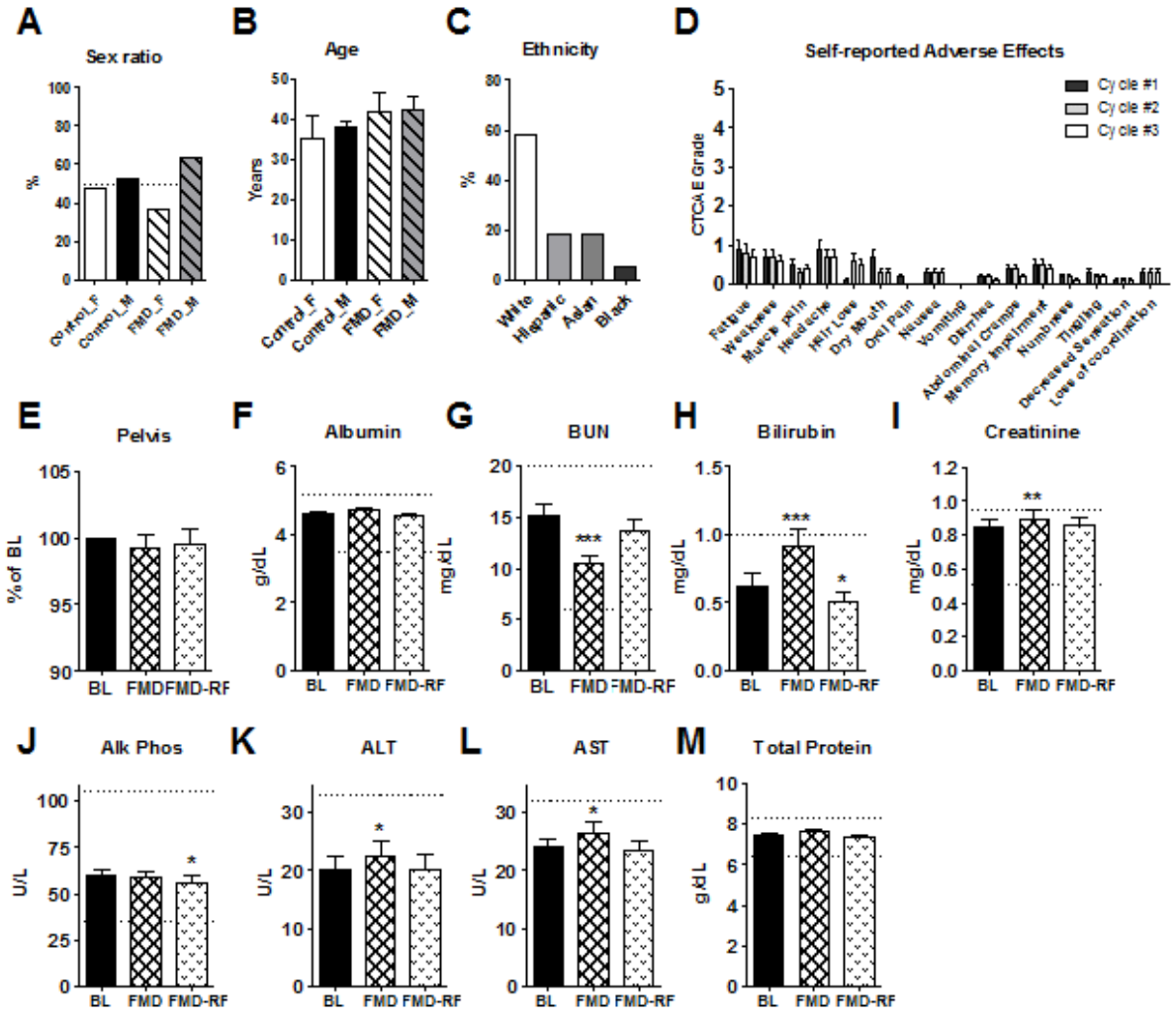

Figure S5 *(Related to Figure 6)*

A) Percentage of female (F) and male (M) participants in the control or FMD groups that were part of a randomized clinical study to evaluate the human FMD version. **B)** Gender specific average age per group. **C)** Ethnic background. **D)** Subject self-reported adverse effects based on Common Terminology Criteria for Adverse Effects (CTCAE; 1 = Mild, 2 = Moderate, 3 = Severe, 4 = Life-threatening, 5 = Death). **E)** Bone mineral density (BMD in g/cm^2; N= 19) was evaluated by dual-energy X-ray absorptiometry and compared to control. Safety and feasibility were evaluated based on complete metabolic panels (**F- M**; N= 19) prior to (Baseline, BL), during (FMD) and after completion of 3 FMD cycles (FMD-RF). All data are expressed as the mean ± SEM.

Table S1 Fasting and the Fasting Mimicking Diet (FMD) induce a similar physiological response in mice. *(Related to Figure 1)*

	Fasting (72 hours)			**FMD (96 hours)**	
	Effect	*Change*	*Reference*	*Effect*	*Change*
Blood glucose	↓	~45%	(Lee et al., 2010; Wang et al., 2006)	↓	~40%
Ketone bodies	↑	~10-fold *	(Shimazu et al., 2013)	↑	~10-fold
IGF-I	↓	~40- 70%	(Brandhorst et al., 2013; Frystyk et al., 1999; Lee et al., 2010)	↓	~45%
IGFBP-1	↑	~7- 11-fold	(Frystyk et al., 1999; Lee et al., 2010)	↑	~8-fold

* after 24 hours of fasting. *Abbreviations*: IGF-I, insulin-like growth factor 1; IGFBP-1, insulin-like growth factor binding protein 1.

Table S2 Overview of autopsy results from the *ad lib* control and Fasting Mimicking Diet (FMD) mouse cohorts. *(Related to Figure 2)*

	Ad lib		FMD	
	Total	%	Total	%
Lymphoma	30	66.7	11	39.3
Liver	**11**	**24.4**	**4**	**14.3**
Lymphocytic infiltration	1	2.2		
Fibrosis	1	2.2	1	3.6
*Necrosis (*with Inflammation)*	2	4.4	1	3.6
Infarct	1	2.2	1	3.6
Congested	3	6.7	1	3.6
Chronic inflammation	2	4.4		
(Diffuse) Acute inflammation	1	2.2		
Spleen	**3**	**6.7**	**3**	**10.7**
Organized thrombus			1	3.6
Infarct	2	4.4	1	3.6
Extensive medullary hematopoiesis	1	2.2		
*Follicular hyperplasia^*			1	3.6
Kidney	**1**	**2.2**	**1**	**3.6**
Cortical cysts			1	3.6
Medullary cyst	1	2.2		
Ovary/ Ovaduct	**5**	**11.1**	**1**	**3.6**
Hemorrhagic cyst	1	2.2		
*Necrosis**			1	3.6
Fibrosis	1	2.2		
Dilated fluid-filled uterine horn	1	2.2		
Calcification	1	2.2		
Cyst attached to uterine horn (benign)	1	2.2		
Urinary bladder	**0**	**0.0**	**1**	**3.6**
Dilated, edematous			1	3.6
Lungs	**1**	**2.2**	**2**	**7.1**
Aspiration pneumonia			2	7.1
Atypical/mitotically active infiltrate#	1	2.2		
Pancreas	**0**	**0.0**	**1**	**3.6**
Granuloma			1	3.6
Lymphnodes	**2**	**4.4**	**0**	**0.0**
Reactive	1	2.2		
Cavernous hemangioma†	1	2.2		
Others	**6**	**13.3**	**0**	**0.0**
Myositis	1	2.2		
Cutaneous hemangioma	1	2.2		
Fibrosarcoma (subcutan)	2	4.4		
Enlarged salivary gland	2	4.4		

Total incidence and percentage is shown per organ (gray rows) and individual abnormality. Lymphoma incidence involves both systemic and localized cases. ^, consistent with chronic inflammation; *, possibly due to torsion; #, consistent with lymphoma; †, associated with chronic inflammation with numerous plasma cells and reactive mast cells.

Table S3 Complete blood counts of young and 20.5 months-old mice. *(Related to Figure 2)*

	4 Month	20.5 month			
	CTRL	**CTRL**		**FMD**	**FMD-RF**
White Blood Cell count (10^9/L)	9.13 ± 0.85	4.49 ± 0.59	^	5.38 ± 0.92	9.90 ± 2.04 †
Lymphocyte count (10^9/L)	6.48 ± 0.49	1.79 ± 0.22	^^^	2.55 ± 0.43 ‡‡	5.31 ± 0.73 †††
Monocyte count (10^9/L)	0.31 ± 0.04	0.47 ± 0.11		0.33 ± 0.14	0.54 ± 0.18
Granulocyte count (10^9/L)	2.32 ± 0.34	2.23 ± 0.50		2.50 ± 0.84	4.04 ± 1.37
Lymphocyte (%)	72.29 ± 1.74	43.09 ± 8.26	^^	51.07 ± 9.27	57.94 ± 6.61
Monocyte (%)	3.34 ± 0.22	10.34 ± 1.70	^^^	6.05 ± 1.18	6.19 ± 2.01
Granulocyte (%)	24.20 ± 1.60	46.57 ± 7.14	^	42.88 ± 8.49	30.76 ± 7.11
Red Blood Cell count (10^9/L)	8.59 ± 0.19	7.10 ± 0.22	^^	8.64 ± 0.34 **, ‡	7.47 ± 0.32
Hemoglobin (g/L)	12.88 ± 0.27	10.57 ± 0.30	^^	13.42 ± 0.57 **, ‡	11.57 ± 0.54
Hematocrit (rel. volume of erythrocytes)	36.23 ± 1.35	30.70 ± 0.94		36.50 ± 1.62 *	32.86 ± 1.24
Mean Corpuscular Volume (fL)	47.42 ± 3.32	43.36 ± 0.62		42.30 ± 0.38	44.10 ± 0.54
Mean Corpuscular Hemoglobin (pg)	14.94 ± 0.05	14.86 ± 0.23		15.47 ± 0.09	15.44 ± 0.12
Mean Corpuscular Hemoglobin Concentration (g/L)	34.84 ± 1.34	34.41 ± 0.49		36.22 ± 0.46 *	35.10 ± 0.39
Red Cell Distribution Width	12.23 ± 0.13	13.57 ± 0.28	^	13.75 ± 0.31	13.99 ± 0.32
Platelet Count (10^9/L)	348.40 ± 13.38	192.90 ± 82.75		712.80 ± 53.82 **, ‡	325.00 ± 124.00
Mean Platelet Volume (fL)	5.38 ± 0.0.	6.10 ± 0.16	^^	5.45 ± 0.19	6.16 ± 0.24
Platelet Distribution Width	14.83 ± 0.05	14.97 ± 0.12		14.70 ± 0.19	15.10 ± 0.12
Plateletcrit	0.18 ± 0.01	0.11 ± 0.05		0.39 ± 0.034 **	0.19 ± 0.07

^ p< 0.05, ^^ p<0.01, ^^^ p<0.001 young (4 months) compared to old (20.5 months); * p< 0.05, ** p<0.01, *** p<0.001 young (4 months) compared to old (20.5 months); † p< 0.05, †† p<0.01, ††† p<0.001 young (4 months) compared to old (20.5 months); ‡ p< 0.05, ‡‡ p<0.01, ‡‡‡ p<0.001 young (4 months) compared to old (20.5 months).

Table S4 Caloric content of the human FMD regimen. *(Related to Figure 6)*

	Day 1	Day 2- 5
Calories	~1090	~725
Protein (%)	10	9
Fat (%)	56	44
Carbohydrates (%)	34	47

Supplemental Experimental Procedures:

Physiological Biomarkers β–hydroxybutyrate was measured with a colorimetric assay kit following the manufacturer's protocol (#700190, Cayman Chemical). Insulin level were measured using a mouse/rat specific ELISA (Millipore, #EZRMI-13K) following the manufacturer's protocol. Human serum IGF-I and IGFBP-1 was measured with an in-house enzyme-linked immunosorbent assay (ELISA) based on paired specific antibodies (R&D Systems) and validated against the commercial kit from Diagnostic Systems Laboratories. CRP levels were measured with a human specific ELISA kit following the manufacturer's protocol (R&D Systems, #DCRP00). Mouse serum IGF-I was measured using a mouse specific ELISA kit (R&D Systems). Mouse serum IGFBP-1 levels were measured by in-house ELISA assays using recombinant mouse proteins and antibodies from R&D Systems (MAB 1240 as capture antibody and BAF 1240 as detection antibody, R&D Systems, Minneapolis, MN, USA) as described previously (Gray et al., 2011). PKA activity was measured using ENZO PKA kinase activity kit (ENZO Lifesciences ADI-EKS-390A). Mouse kidney function was evaluated by serum creatinine and blood urea nitrogen (BUN) at 16.5, 22 and 27 months of age based on a quantitative colorimetric assay (Quantichrome^{TM}; DICT-500 and DIUR-500, respectively) following the manufacturer's protocol (BioAssay Systems). In brief, 30 µl serum (for creatinine) or 5 µl (for BUN) and 200 µl working solution were added into a 96 well plate. Mouse liver function was analyzed by measuring serum alanine transaminase (EnzyChrom^{TM}; EALT-100) following the manufacturer's protocol (BioAssay Systems). In brief, 20 µl serum and 200 µl working solution were added into a 96 well plate.

X-ray computed tomography (CT)-Scans *(continued)* CT phantoms for density calibration were used to fit data and determine the slope and intercept. Images were reconstructed and densities calculated based on the phantom scan values. The slope and intercept of the phantoms were used to interpolate/extrapolate the tissue mineral density (TMD) for the femur of all animals. The reported tissue mineral density of the investigated bone volume contains hydroxyapatite contribution from both the cortical and trabecular bone.

The body fat composition was measured *in vivo* for N=3/group. The abdominal region of each mouse was scanned with a Siemens InveonCT scanner at the following settings: 80 kV, 250 µA, 220° total rotation in 180 rotation steps, binning of 4 and 300 ms exposure time. Two-dimensional gray-scale image slices were reconstructed into a three-dimensional tomography. Scans were reconstructed between the proximal end of L1 and the distal end of L5 using COBRA software. The region of interest for each animal was defined based on skeletal landmarks from gray-scale images. To analyze total fat volume, a threshold segmenting fat from other tissues and background was determined by *ex vivo* microCT imaging of a freshly harvested fat pad, muscle and liver tissue from a C57BL/6J mouse. The abdominal muscular wall was used as the demarcation line to separate visceral adipose tissue from subcutaneous adipose tissue. Fat scans by means of microCT were performed 5 days following refeeding to avoid interferences during the immediate recovery time from the FMD.

Immunohistochemistry Adult mice were anesthetized with isoflurane and intracardially perfused with saline followed by 4% paraformaldehyde (PFA). The tissues were removed immediately and post-fixed in 4% PFA for 24 hours and stored in 0.05% sodium azide. Brain was cut sagittally (40 µm), and stored in 0.05% sodium azide solution. Briefly, the sections were rinsed 3 times in

phosphate buffered saline (PBS) for 5 minutes and denatured in 2N HCl at 37°C for 20 minutes. Sections were neutralized with 0.1M boric acid for 10 minutes and blocked with 2% Normal Donkey Serum (NDS; Jackson ImmunoResearch) for 1 hour at room temperature. For liver, samples were obtained from the right lobe and processed for paraffin embedding and sectioning at the USC Stem Cell Core. Hepatic proliferation was assessed by Ki67 (Santa Cruz) staining on days 1, 3 and 7 post refeeding following the BrdU protocol. For the evaluation of adult neurogenesis in the hippocampus, sections were incubated in BrdU (Serotec, 1:200), doublecortin (Santa Cruz, 1:200), GFAP (Cell Signaling, 1:200), Sox2 (Millipore, 1:100), diluted in 2% NDS in 0.3% triton overnight at 4°C. The sections were rinsed 3 times in PBS for 10 min, incubated in anti-rat IgG tagged with Alexa Flour488 and anti-goat IgG tagged with Alexa Flour598 (Invitrogen, 1:400) diluted in 2% NDS. Sections are mounted using Vectashield (Vector). Free-floating hippocampal (one out of every 6^{th}) were processed for fluorescent immunohistochemistry. Co-expression was confirmed by fluorescent- and confocal-microscopy. Ki67-positive cells were quantified by averaging at least 5 consecutive, non-overlapping image frames from at least two tissue sections 30 μm apart. Digital images were collected on a Leica SL confocal microscope located at the Multiphoton Imaging Core of the University of Southern California. For quantification, serological counting methods were used.

Western blotting *(continued)* About 50 mg of muscle (*m. gastrocnemius*) was homogenized in 80 mM Tris-HCl, pH 6.8, containing 100 mM DTT, 70 mM SDS, and 1 mM glycerol, with freshly added protease and phosphatase inhibitor cocktails, kept on ice for 30 min, centrifuged at 15000 x g for 10 min at 4°C, and the supernatant was collected. Protein concentration was assayed using BSA as working standard. Equal amounts of protein (30 μg) were heat-denaturized in sample-

loading buffer (50 mM Tris-HCl, pH 6.8, 100 mM DTT, 2% SDS, 0.1% bromophenol blue, 10% glycerol), resolved by SDS-PAGE and transferred to nitrocellulose membranes (Bio-Rad, Hercules, CA, USA). The filters were blocked with Tris-buffered saline (TBS) containing 0.05% Tween and 5% non-fat dry milk and then incubated overnight with antibodies directed against MyoD, and myogenin (Santa Cruz Biotechnology, CA, USA), the monoclonal antibody against Pax7 (developed by Atsushi Kawakami, obtained from the Developmental Studies Hybridoma Bank (University of Iowa)) and LC3B (L7583; BD Biosciences, San Jose, CA). Peroxidase-conjugated IgG (Bio-Rad, Hercules, CA, USA) was used as secondary antibody. Membrane-bound immune complexes were detected by an enhanced chemiluminescence system (Santa Cruz Biotechnology, USA) on a photon-sensitive film (Hyperfilm ECL, GE Healthcare, Milano, Italy). Protein loading was normalized according to tubulin or GAPDH expression. Quantification was performed by densitometric analysis using TotalLab software (NonLinear Dynamics, Newcastle upon Tyne, UK).

Quantitative PCR Relative transcript expression levels were measured using a SYBR Green-based method. IGF1R F-CAAGCTGTGTGTCTCCGAAA/R-CTCCGTTGTTCCTGGTGTTT and NeuroD1 F-ATTGCGTTGCCTTAGCACTT/R-TGCATTTCGGTTTTCATCCT. Average fold changes were calculated by differences in threshold cycles (Ct) between pairs of samples.

Behavior Studies *(continued)* To prevent starvation-induced hyper-activity (e.g. foraging associated movement (personal observation SB)), FMD animals were exposed to the behavior tests not earlier than 3 days after re-feeding. Y-maze Short-term spatial recognition memory was examined by a spatial novelty preference task in the Y- maze. The Y- maze was made of black

plexiglas and comprised three identical arms (50 × 9 × 10 cm), radiating from a central triangle (8 cm on each side) and spaced 120° apart from each other. The test started placing the rodent in one of the arms of the maze. The mouse was allowed to freely explore the environment for 8 minutes and the total numbers of arm entries and arm choices were recorded. Arm choices are defined as both fore-paws and hind-paws fully entering the arm. We used an Accelerating rotarod consisting of a 3 cm diameter rotating rod (suspended 15 cm above the base) and divided by flanges so that up to 5 mice could be tested simultaneously. Mice were placed on the rotating rod and the speed gradually increased from 4 rpm to 40 rpm within a 5 min session. The exact speed at which the mice fell off and time that the mice were able to stay on the bar were recorded. On two consecutive days, the mice were given three successive trials, for a total of six trials. Novel Object Recognition The novel object recognition test was introduced to assess the ability of rodents to recognize a novel object in a familiar environment. The test includes a habituation phase (5 min on day one) and trial phases (5 min each on the second day) for each mouse. Briefly, in the habituation phase, the mouse was placed into a rectangular cage (50 x 50 x 40 cm) made of black acryl plexiglas for 5 min on day one without any object. The testing session comprised two trials with the duration of each trial being 5 min. Mice were always placed in the apparatus facing the wall at the middle of the front segment. Exploration of the objects is defined as any physical contact with an object (whisking, sniffing, rearing on or touching the object) as well as positioning its nose toward the object at a distance of less than 2 cm; however, sitting or standing on top of the object is not counted toward the exploration time. After the first exploration period, the mice were placed back in their home cage. To control for odor cues, the open field arena and the objects were thoroughly cleaned with water, dried, and ventilated for a few minutes between mice. After a 1 hour delay interval, mice were placed back in the apparatus for the second trial (T2), but now with two

dissimilar objects, a familiar one and a new one. Barnes Maze The maze consists of a platform with 20 holes (San Diego Instruments) and 20 boxes underneath each hole; with only one hole big enough to allow the entire mouse to enter/hide (escape box, ”EB”). A unique position for the EB was randomly assigned to each mouse; this position was always located underneath the same hole for a specific animal. In order to minimize the inter-maze cues, the platform was rotated after each trial. All mice were trained once daily on days 0 to 7. During training sessions, mice were allowed to freely explore the maze until either entering the EB or after 2 min time elapsed. If the mouse did not enter the EB by itself, it was gently guided to and allowed to stay in the EB for 30 seconds. After the training session, mice were tested twice daily for 7 days. Testing was similar to training, but if after 2 min the mouse did not find the EB, it was directly returned to its cage.